SIAM J. NUMER. ANAL.
Vol. 34, No. 6, pp. 2456–2481, December 1997

021

ON SOR WAVEFORM RELAXATION METHODS*

JAN JANSSEN† AND STEFAN VANDEWALLE‡

Abstract. Waveform relaxation is a numerical method for solving large-scale systems of ordinary differential equations on parallel computers. It differs from standard iterative methods in that it computes the solution on many time levels or along a continuous time interval simultaneously. This paper deals with the acceleration of the standard waveform relaxation method by successive overrelaxation (SOR) techniques. In particular, different SOR acceleration schemes, based on multiplication with a scalar parameter or convolution with a time-dependent function, are described and theoretically analyzed. The theory is applied to a one-dimensional and two-dimensional model problem and checked against results obtained by numerical experiments.

Key words. waveform relaxation, successive overrelaxation, convolution

AMS subject classifications. 65F10, 65L05

PII. S0036142995294292

1. Introduction.

Waveform relaxation, also called dynamic iteration or Picard–Lindelöf iteration, is a highly parallel iterative method for numerically solving large-scale systems of ordinary differential equations (ODEs). It is the natural extension to systems of differential equations of the relaxation methods for solving systems of algebraic equations. In the present paper we will concentrate on linear ODE systems of the form

$$B\dot{u}(t) + Au(t) = f(t), \quad u(0) = u_0, \tag{1.1}$$

where the matrices B and A belong to $\mathbb{C}^{d\times d}$, and B is assumed to be nonsingular. Such a system is found, for example, after spatial discretization of a constant-coefficient parabolic partial differential equation (PDE) using a conforming Galerkin finite-element method [23]. Matrix B is then a symmetric positive definite mass matrix and A is a stiffness matrix. A spatial discretization based on finite volumes or finite differences leads to a similar system with B, respectively, a diagonal matrix or the identity matrix. Waveform relaxation has been applied successfully to more general, time-dependent coefficient problems and to nonlinear problems. Yet, only problems of the form (1.1) seem to allow precise quantitative convergence estimates of the waveform iteration.

Waveform relaxation methods for linear problems (1.1) are usually defined by splittings of the coefficient matrices of the ODE, i.e., $B = M_B - N_B$ and $A = M_A - N_A$, and correspond to an iteration of the following form:

$$\left(M_B\frac{d}{dt} + M_A\right)u^{(\nu)}(t) = \left(N_B\frac{d}{dt} + N_A\right)u^{(\nu-1)}(t) + f(t), \quad u^{(\nu)}(0) = u_0. \tag{1.2}$$

*Received by the editors November 1, 1995; accepted for publication (in revised form) July 18, 1996.

http://www.siam.org/journals/sinum/34-6/29429.html

†Katholieke Universiteit Leuven, Department of Computer Science, Celestijnenlaan 200A, B-3001 Heverlee, Belgium (jan.janssen@cs.kuleuven.ac.be). This text presents research results of the Belgian Incentive Program "Information Technology" – Computer Science of the Future, initiated by the Belgian State – Prime Minister's Service – Federal Office for Scientific, Technical and Cultural Affairs. The scientific responsibility is assumed by its authors.

‡California Institute of Technology, Applied Mathematics 217-50, Pasadena, CA 91125 (vandewalle@na-net.ornl.gov). This work was supported in part by the NSF under Cooperative Agreement CCR-9120008.

In [8], we have investigated the convergence of the above iteration, when (M_B, N_B) and (M_A, N_A) correspond to a standard Jacobi or Gauss–Seidel matrix splitting. In that paper we assumed the resulting ODEs were solved exactly, i.e., the iteration is continuous in time. In [9] a similar iteration was studied for the discrete-time case, defined by discretizing (1.2) with a linear multistep method. The Jacobi and Gauss–Seidel waveform methods proved to be convergent, with convergence rates very similar to the convergence rates obtained with corresponding relaxation methods for algebraic systems. In order to improve the convergence of the waveform relaxation methods, several acceleration techniques have been described: successive overrelaxation [1], [2], [17], [18], [21], Chebyshev iteration [13], [22], Krylov subspace acceleration [15], and multigrid acceleration [8], [9], [14], [24].

This paper deals with acceleration methods based on the SOR idea. A first SOR waveform relaxation method, based on matrix splitting, was introduced by Miekkala and Nevanlinna in [17], [18] for problems of the form (1.1) with $B = I$. They showed that SOR leads to some acceleration, although a much smaller one than the acceleration by the standard SOR method for algebraic equations. A second method, briefly discussed in [21], is based on multiplying the Gauss–Seidel correction by an overrelaxation parameter. As in the case of the previous method, numerical experiments indicate that a careful selection of the overrelaxation parameter leads to some acceleration, but again only a marginal one. These somewhat disappointing results led Reichelt, White, and Allen to define a third method, which they named the *convolution SOR* waveform relaxation method [21]. They changed the second SOR algorithm by replacing the multiplication with an SOR parameter by a convolution with a time-dependent SOR kernel. This fix appeared to be a very effective one. Application to a nonlinear semiconductor device simulation problem showed the new method to be by far superior to the standard SOR waveform relaxation method.

In this paper, we extend the SOR waveform relaxation techniques to general problems of the form (1.1). Using the theoretical framework developed in [8], [9], the convergence properties of these methods are investigated. A lot of attention is hereby paid to the convolution SOR method, the discrete-time convergence properties of which were outlined for the $B = I$ case in [21]. We complete this discrete-time analysis and also treat the continuous-time case. We identify the nature of the different continuous-time and discrete-time SOR iteration operators, and derive the corresponding spectral radii and norm expressions. Application of these results to some model problems yields explicit formulae for the optimal convergence factors as a function of the mesh size h. These results are verified by numerical experiments. In particular, we show that for these model problems the convolution SOR waveform method attains an identical acceleration as the standard SOR method does for the linear system $Au = f$. This is not so for the other SOR waveform methods. We also illustrate by numerical experiments that the convolution SOR algorithm can attain excellent convergence rates, even in cases where the current theory does not apply. The structure of the paper is as follows. We start in section 2 by describing the different types of SOR waveform algorithms. Their convergence as continuous-time methods is presented in section 3. In section 4, we briefly point out the corresponding discrete-time convergence results, and we show how the latter relate to the continuous-time ones. A model problem analysis and numerical results for the one- and two-dimensional heat equation are given for point relaxation in section 5 and for line relaxation in section 6. Finally, we end in section 7 with some concluding remarks.

2. SOR waveform relaxation methods.

2.1. Continuous-time methods. The most obvious way to define an SOR waveform method for systems of differential equations is based on the natural extension of the standard SOR procedure for algebraic equations [25], [27]. Let the elements of matrices B and A be denoted by b_{ij} and a_{ij}, $1 \leq i, j \leq d$. First, a function $\hat{u}_i^{(\nu)}(t)$ is computed with a Gauss–Seidel waveform relaxation scheme,

$$\begin{aligned} \left(b_{ii}\frac{d}{dt} + a_{ii}\right)\hat{u}_i^{(\nu)}(t) &= -\sum_{j=1}^{i-1}\left(b_{ij}\frac{d}{dt} + a_{ij}\right)u_j^{(\nu)}(t) \\ &\quad - \sum_{j=i+1}^{d}\left(b_{ij}\frac{d}{dt} + a_{ij}\right)u_j^{(\nu-1)}(t) + f_i(t), \end{aligned} \tag{2.1}$$

with $\hat{u}_i^{(\nu)}(0) = (u_0)_i$. Next, the old approximation $u_i^{(\nu-1)}(t)$ is updated by multiplying the correction $\hat{u}_i^{(\nu)}(t) - u_i^{(\nu-1)}(t)$ using an overrelaxation parameter ω,

$$u_i^{(\nu)}(t) = u_i^{(\nu-1)}(t) + \omega \cdot \left(\hat{u}_i^{(\nu)}(t) - u_i^{(\nu-1)}(t)\right). \tag{2.2}$$

Elimination of the intermediate approximation $\hat{u}_i^{(\nu)}(t)$ from (2.1) and (2.2) leads to an iterative scheme of the form (1.2), corresponding to the matrix splittings

$$M_B = \frac{1}{\omega}D_B - L_B, \quad N_B = \frac{1-\omega}{\omega}D_B + U_B \tag{2.3}$$

and

$$M_A = \frac{1}{\omega}D_A - L_A, \quad N_A = \frac{1-\omega}{\omega}D_A + U_A, \tag{2.4}$$

where $B = D_B - L_B - U_B$ and $A = D_A - L_A - U_A$ are the standard splittings of B and A in diagonal, lower and upper triangular parts [8, Rem. 3.1]. This method was briefly considered for ODE systems (1.1) with $B = I$ in [21]. Its nonlinear variant was studied in [1], [2].

The first step of the *convolution SOR waveform relaxation* (CSOR) method is similar to the first step of the previous scheme, and consists of the computation of a Gauss–Seidel iterate $\hat{u}_i^{(\nu)}(t)$ using (2.1). Instead of multiplying the resulting correction by a scalar ω, as in (2.2), the correction is convolved with a function $\Omega(t)$ [21],

$$u_i^{(\nu)}(t) = u_i^{(\nu-1)}(t) + \int_0^t \Omega(t-s) \cdot \left(\hat{u}_i^{(\nu)}(s) - u_i^{(\nu-1)}(s)\right) ds. \tag{2.5}$$

We will allow for fairly general convolution kernels of the form

$$\Omega(t) = \omega\,\delta(t) + \omega_c(t), \tag{2.6}$$

with ω a scalar parameter, $\delta(t)$ the delta function, and $\omega_c(t)$ a function in L_1. In that case, (2.5) can be rewritten as

$$\begin{aligned} u_i^{(\nu)}(t) &= u_i^{(\nu-1)}(t) + \omega \cdot \left(\hat{u}_i^{(\nu)}(t) - u_i^{(\nu-1)}(t)\right) \\ &\quad + \int_0^t \omega_c(t-s) \cdot \left(\hat{u}_i^{(\nu)}(s) - u_i^{(\nu-1)}(s)\right) ds. \end{aligned} \tag{2.7}$$

The latter equation corresponds to (2.2) with an additional correction based on a Volterra convolution. As such, the standard SOR waveform relaxation method can be treated as a special case of the CSOR method by setting $\omega_c(t) \equiv 0$.

Remark 2.1. The original SOR waveform method, developed and analyzed by Miekkala and Nevanlinna for systems of ODEs (1.1) with $B = I$ in [17], [18] differs from the standard SOR waveform method described above in that only the coefficient matrix A is split in an SOR manner. To distinguish between both SOR methods, we will further refer to the Miekkala–Nevanlinna method as the *single-splitting SOR waveform relaxation* (SSSOR) method, whereas the standard SOR method will be referred to as the *double-splitting SOR* (DSSOR) method. The SSSOR method, which can be cast into the double-splitting framework of (1.2) by setting $M_B = I$, $N_B = 0$, and (2.4), has not yet found any use for general ODE systems (1.1) with $B \neq I$. Hence, in that case we will distinguish only between the CSOR method and its variant for $\omega_c(t) \equiv 0$, i.e., the standard SOR or DSSOR method.

2.2. Discrete-time methods. In an actual implementation, the continuous-time methods are replaced by their discrete-time variants. As in [9], we shall concentrate in this paper on the use of (irreducible, consistent, zero-stable) linear multistep formulae for time discretization. For the reader's convenience, we recall the general linear multistep formula for calculating the solution to the ODE $\dot{y}(t) = f(t, y)$ with $y(0) = y[0]$, see e.g. [12, p. 11],

$$\frac{1}{\tau} \sum_{l=0}^{k} \alpha_l y[n+l] = \sum_{l=0}^{k} \beta_l f[n+l].$$

In this formula, α_l and β_l are real constants, τ denotes a constant step size, and $y[n]$ denotes the discrete approximation of $y(t)$ at $t = n\tau$. We shall assume that k starting values $y[0], y[1], \ldots, y[k-1]$ are given. The characteristic polynomials of the linear multistep method are given by

$$a(z) = \sum_{l=0}^{k} \alpha_l z^l \quad \text{and} \quad b(z) = \sum_{l=0}^{k} \beta_l z^l.$$

The stability region S consists of those $\mu \in \bar{\mathbb{C}}$ for which the polynomial $a(z) - \mu b(z)$ (around $\mu = \infty$: $\mu^{-1}a(z) - b(z)$) satisfies the root condition: all roots satisfy $|z_l| \leq 1$ and those of modulus 1 are simple.

The first step of the *discrete-time convolution SOR waveform relaxation* algorithm is obtained by discretizing (2.1). The second step approximates the convolution integral in (2.5) by a convolution sum with kernel $\Omega_\tau = \{\Omega[n]\}_{n=0}^{N-1}$, where N denotes the (possibly infinite) number of time steps,

$$u_i^{(\nu)}[n] = u_i^{(\nu-1)}[n] + \sum_{l=0}^{n} \Omega[n-l] \cdot \left(\hat{u}_i^{(\nu)}[l] - u_i^{(\nu-1)}[l] \right). \tag{2.8}$$

We obtain from this a discrete-time analogue of (2.7) if we set $\Omega_\tau = \omega\delta_\tau + (\omega_c)_\tau$, with δ_τ the discrete delta function [20, p. 409]. The right-hand side of (2.8) then becomes

$$u_i^{(\nu-1)}[n] + \omega \cdot \left(\hat{u}_i^{(\nu)}[n] - u_i^{(\nu-1)}[n] \right) + \sum_{l=0}^{n} \omega_c[n-l] \cdot \left(\hat{u}_i^{(\nu)}[l] - u_i^{(\nu-1)}[l] \right).$$

Note that the convolution sum is a bounded operator if Ω_τ (or $(\omega_c)_\tau$) is an l_1-sequence. Clearly, the discrete-time analogue to the standard SOR waveform relaxation method is obtained by setting $\omega_c[n] \equiv 0$. The latter can also be derived by discretizing (1.2) and using the splittings (2.3) and (2.4).

We shall always assume that we do not iterate on k given starting values, i.e., $\hat{u}_i^{(\nu)}[n] = u_i^{(\nu)}[n] = u_i^{(\nu-1)}[n] = u_i[n]$, $n < k$. For implicit multistep methods, i.e., methods with $\beta_k \neq 0$, the linear systems arising from discretizing (1.2) can be solved uniquely for every n if and only if the discrete solvability condition,

$$\frac{\alpha_k}{\beta_k} \notin \sigma(-\tau M_B^{-1} M_A),$$

is satisfied, where $\sigma(\cdot)$ denotes the spectrum [9, Eq. (4.5)]. In the case of (2.1), this simplifies to

$$\frac{\alpha_k}{\beta_k} \notin \sigma(-\tau D_B^{-1} D_A). \tag{2.9}$$

2.3. Blockwise methods. The pointwise SOR waveform relaxation methods described above can be adapted easily to the *blockwise* relaxation case. Matrices B and A are then partitioned into similar systems of $d_b \times d_b$ rectangular blocks b_{ij} and a_{ij}. Correspondingly, D_B, L_B, and U_B (and D_A, L_A, and U_A) are *block* diagonal, *block* lower triangular, and *block* upper triangular matrices.

3. Continuous-time convergence analysis. We will analyze the convergence properties of the continuous-time SOR waveform relaxation methods outlined in the previous section. We will consider the general case of blockwise relaxation, which includes pointwise relaxation as a limiting case. This analysis will follow the framework of [8] and extend and complete the results of [21] to systems of the form (1.1). We will concentrate on deriving the nature and the properties of the iteration operator of the CSOR waveform relaxation method. The results for the standard SOR waveform method then follow immediately by setting $\omega_c(t) \equiv 0$. For the splitting SOR waveform method with single splitting—which finds use only in the $B = I$ case—we refer to [17], [18].

3.1. Nature of the operator. In order to identify the nature of the CSOR waveform iteration operator we need the following elementary result, which we formulate as a lemma.

LEMMA 3.1. *The solution to the ODE* $b\dot{u}(t) + au(t) = q\dot{v}(t) + pv(t) + w(t)$ *with constants* $b, a, q, p \in \mathbb{C}^{m\times m}$ *and* b *nonsingular, is given by* $u(t) = \mathcal{K}v(t) + \varphi(t)$, *with*

$$\mathcal{K}x(t) = b^{-1}qx(t) + \int_0^t k_c(t-s)x(s)ds \quad \text{with} \quad k_c(t) = e^{-b^{-1}at}b^{-1}(p - ab^{-1}q),$$

$$\varphi(t) = e^{-b^{-1}at}\left(u(0) - b^{-1}q\,v(0)\right) + \int_0^t e^{-b^{-1}a(t-s)}b^{-1}w(s)ds.$$

The function $k_c(t) \in L_1(0,\infty)$ *if* $\mathrm{Re}(\lambda) > 0$ *for all* $\lambda \in \sigma(b^{-1}a)$. *If, in addition,* $w(t) \in L_p(0,\infty)$, *then* $\varphi(t) \in L_p(0,\infty)$.

Proof. The lemma is an immediate consequence of the well-known solution formula for the ODE $\dot{u} + au = f$, see e.g. [4, p. 119]. ∎

The CSOR waveform relaxation algorithm implicitly defines a classical successive iteration scheme of the form $u^{(\nu)}(t) = \mathcal{K}^{CSOR}u^{(\nu-1)}(t) + \varphi^{CSOR}(t)$, where $\varphi^{CSOR}(t)$

depends on the ODE's right-hand side $f(t)$ and the initial condition, and where $\mathcal{K}^{CSOR}$ denotes a linear operator, which we name the continuous-time CSOR waveform relaxation operator. The nature of this operator is identified in the next theorem.

THEOREM 3.2. *The continuous-time convolution SOR waveform relaxation operator is of the form*

$$\mathcal{K}^{CSOR} = K^{CSOR} + \mathcal{K}_c^{CSOR}, \tag{3.1}$$

with $K^{CSOR} \in \mathbb{C}^{d\times d}$ *and with* $\mathcal{K}_c^{CSOR}$ *a linear Volterra convolution operator, whose matrix-valued kernel* $k_c^{CSOR}(t) \in L_1(0,\infty)$ *if all eigenvalues of* $D_B^{-1}D_A$ *have positive real parts and if* $\Omega(t)$ *is of the form* (2.6) *with* $\omega_c(t) \in L_1(0,\infty)$.

Proof. Introductory Lemma 3.1 can be applied to equation (2.1) to give

$$\hat{u}_i^{(\nu)}(t) = \sum_{j=1}^{i-1}(H_{ij} + (h_c)_{ij}\star)u_j^{(\nu)}(t) + \sum_{j=i+1}^{d_b}(H_{ij} + (h_c)_{ij}\star)u_j^{(\nu-1)}(t) + \phi_i(t). \tag{3.2}$$

Here, we have used the symbol "$\star$" to denote convolution. The (matrix) constants H_{ij} and (matrix) functions $(h_c)_{ij}(t)$ can be derived from the result of Lemma 3.1 with $b = b_{ii}$, $a = a_{ii}$, $q = -b_{ij}$, and $p = -a_{ij}$. Note that $(h_c)_{ij}(t) \in L_1(0,\infty)$ if $\mathrm{Re}(\lambda)$ is positive for all $\lambda \in \sigma(b_{ii}^{-1}a_{ii})$, while $\phi_i(t) \in L_p(0,\infty)$ if, in addition, $f_i(t) \in L_p(0,\infty)$.

We shall prove the existence of constants K_{ij}^{CSOR} and L_1-functions $(k_c^{CSOR})_{ij}(t)$, $i,j = 1,\ldots,d_b$, such that

$$u_i^{(\nu)}(t) \;=\; \sum_{j=1}^{d_b} K_{ij}^{CSOR}u_j^{(\nu-1)}(t) \;+\; \sum_{j=1}^{d_b}(k_c^{CSOR})_{ij} \star u_j^{(\nu-1)}(t) \;+\; \varphi_i(t). \tag{3.3}$$

The case $i = 1$ follows immediately from the combination of (3.2) with (2.7). More precisely, $K_{11}^{CSOR} = (1-\omega)I$, $K_{1j}^{CSOR} = \omega H_{1j}$, $(k_c^{CSOR})_{11}(t) = -\omega_c(t)I$, $(k_c^{CSOR})_{1j}(t) = \omega\,(h_c)_{1j}(t) + \omega_c\star(H_{1j} + (h_c)_{1j})(t)$, $2 \le j \le d_b$, and $\varphi_1(t) = (\Omega\star\phi_1(t))I$ with I the identity matrix whose dimension equals the dimension of b_{11} and a_{11}.

The general case follows by induction on i. This step involves computing $u_i^{(\nu)}(t)$ from (3.2) and (2.7) and using (3.3) to substitute $u_j^{(\nu)}(t)$, $j < i$. The result then follows from the knowledge that linear combinations and convolutions of L_1-functions are in L_1. ∎

3.2. Symbol. The symbol $\mathbf{K^{CSOR}}(z)$ of the continuous-time CSOR waveform relaxation operator is obtained after Laplace-transforming the iterative scheme (2.1)–(2.5). This gives the equation $\tilde{u}^{(\nu)}(z) = \mathbf{K^{CSOR}}(z)\tilde{u}^{(\nu-1)}(z) + \tilde{\varphi}(z)$ in Laplace-transform space, where we have used the "˜"-notation to denote a Laplace-transformed variable, as, for instance, in $\tilde{u}^{(\nu)}(z) = \mathcal{L}\left(u^{(\nu)}(t)\right) = \int_0^\infty u^{(\nu)}(t)e^{-zt}dt$. In particular, we obtain

$$\begin{aligned}\mathbf{K^{CSOR}}(z) = &\left(z\left(\frac{1}{\tilde{\Omega}(z)}D_B - L_B\right) + \left(\frac{1}{\tilde{\Omega}(z)}D_A - L_A\right)\right)^{-1} \\ &\cdot\left(z\left(\frac{1-\tilde{\Omega}(z)}{\tilde{\Omega}(z)}D_B + U_B\right) + \left(\frac{1-\tilde{\Omega}(z)}{\tilde{\Omega}(z)}D_A + U_A\right)\right),\end{aligned} \tag{3.4}$$

where $\tilde{\Omega}(z) = \omega + \tilde{\omega}_c(z)$. With reference to (3.1), we can also write (3.4) as $\mathbf{K^{CSOR}}(z) = K^{CSOR} + \mathbf{K_c^{CSOR}}(z)$, with $\mathbf{K_c^{CSOR}}(z) = \mathcal{L}\left(k_c^{CSOR}(t)\right)$.

3.3. Spectral radii and norm. The convergence properties of the continuous-time CSOR waveform relaxation operator can be expressed in terms of its symbol, as explained in our general theoretical framework for operators consisting of a matrix multiplication and convolution part [8, section 2].

3.3.1. Finite time intervals. The following theorem follows immediately from [8, Lem. 2.1], applied to $\mathcal{K}^{CSOR}$, taking into account that $\omega_c(t)$ is an L_1-function, and, consequently, $\lim_{z\to\infty} \tilde{\omega}_c(z) = 0$.

THEOREM 3.3. *Consider $\mathcal{K}^{CSOR}$ as an operator in $C[0,T]$. Then, $\mathcal{K}^{CSOR}$ is a bounded operator and*

$$\rho\left(\mathcal{K}^{CSOR}\right) = \rho\left(\mathbf{K^{CSOR}}(\infty)\right) = \rho\left(K^{CSOR}\right). \tag{3.5}$$

If $\Omega(t)$ is of the form (2.6) with $\omega_c(t) \in L_1(0,T)$, we have

$$\rho\left(\mathcal{K}^{CSOR}\right) = \rho\left(\left(\frac{1}{\omega}D_B - L_B\right)^{-1}\left(\frac{1-\omega}{\omega}D_B + U_B\right)\right). \tag{3.6}$$

As a result, we have shown that the *asymptotic* convergence behavior of the iteration on a finite time window is independent of the L_1-function $\omega_c(t)$.

3.3.2. Infinite time intervals. If all eigenvalues of $D_B^{-1}D_A$ have positive real parts, Theorem 3.2 implies that the convolution kernel of $\mathcal{K}^{CSOR}$ belongs to $L_1(0,\infty)$. Consequently, we can apply [8, Lems. 2.3 and 2.4] in order to obtain the following convergence theorem.

THEOREM 3.4. *Assume all eigenvalues of $D_B^{-1}D_A$ have positive real parts, and let $\Omega(t)$ be of the form (2.6) with $\omega_c(t) \in L_1(0,\infty)$. Consider $\mathcal{K}^{CSOR}$ as an operator in $L_p(0,\infty)$, $1 \le p \le \infty$. Then, $\mathcal{K}^{CSOR}$ is a bounded operator and*

$$\rho(\mathcal{K}^{CSOR}) = \sup_{Re(z)\ge 0} \rho\left(\mathbf{K^{CSOR}}(z)\right) = \sup_{\xi\in\mathbb{R}} \rho\left(\mathbf{K^{CSOR}}(i\xi)\right). \tag{3.7}$$

Denote by $||\cdot||_2$ the L_2-norm and by $||\cdot||$ the standard Euclidean vector norm. Then,

$$||\mathcal{K}^{CSOR}||_2 = \sup_{Re(z)\ge 0} ||\mathbf{K^{CSOR}}(z)|| = \sup_{\xi\in\mathbb{R}} ||\mathbf{K^{CSOR}}(i\xi)||. \tag{3.8}$$

Remark 3.1. In Theorem 3.4, we require $\tilde{\Omega}(z)$ to be the Laplace transform of a function of the form (2.6) with $\omega_c(t) \in L_1(0,\infty)$. For this, a sufficient (but not necessary) condition is that $\tilde{\Omega}(z)$ is a bounded and analytic function in an open domain containing the closed right half of the complex plane [10, Prop. 2.3].

3.4. On the relation between the Jacobi and CSOR symbols. At the heart of classical SOR theories for determining the optimal overrelaxation parameter lies usually the existence of a *Young* relation, i.e., a relation between the eigenvalues of the Jacobi and the SOR iteration matrices. The following lemma reveals the existence of such a relation between the eigenvalues of the CSOR symbol $\mathbf{K^{CSOR}}(z)$ and the eigenvalues of the Jacobi symbol

$$\mathbf{K^{JAC}}(z) = (zD_B + D_A)^{-1}(z(L_B + U_B) + (L_A + U_A)). \tag{3.9}$$

It uses the notion of a *block-consistent* ordering, for which we refer to [27, p. 445, Def. 3.2].

LEMMA 3.5. *Assume the matrices B and A are such that $zB + A$ is a block-consistently ordered matrix with nonsingular diagonal blocks, and $\tilde{\Omega}(z) \neq 0$. If $\mu(z)$ is an eigenvalue of $\mathbf{K^{JAC}}(z)$ and $\lambda(z)$ satisfies*

$$(\lambda(z) + \tilde{\Omega}(z) - 1)^2 = \lambda(z)(\tilde{\Omega}(z)\mu(z))^2, \tag{3.10}$$

then $\lambda(z)$ is an eigenvalue of $\mathbf{K^{CSOR}}(z)$. Conversely, if $\lambda(z) \neq 0$ is an eigenvalue of $\mathbf{K^{CSOR}}(z)$ which satisfies (3.10)*, then $\mu(z)$ is an eigenvalue of $\mathbf{K^{JAC}}(z)$.*

Proof. Using the shorthands $D^\star = zD_B + D_A$, $L^\star = zL_B + L_A$, and $U^\star = zU_B + U_A$, we can write (3.9) and (3.4) as

$$\begin{aligned}\mathbf{K^{JAC}}(z) &= (D^\star)^{-1}(L^\star + U^\star),\\ \mathbf{K^{CSOR}}(z) &= (D^\star - \tilde{\Omega}(z)L^\star)^{-1}((1 - \tilde{\Omega}(z))D^\star + \tilde{\Omega}(z)U^\star).\end{aligned}$$

Thus, if $\tilde{\Omega}(z)$ is viewed as a complex overrelaxation parameter, then $\mathbf{K^{JAC}}(z)$ and $\mathbf{K^{CSOR}}(z)$ are the standard Jacobi and SOR iteration matrices for the matrix $zB + A = D^\star - L^\star - U^\star$. The result of the lemma then follows immediately from classical SOR theory [25, Thm. 4.3], [27, p. 451, Thm. 3.4]. ∎

Under the assumption of a block-consistent ordering of $zB + A$, we have that if $\mu(z)$ is an eigenvalue of $\mathbf{K^{JAC}}(z)$ then also $-\mu(z)$ is an eigenvalue of $\mathbf{K^{JAC}}(z)$, see e.g. [27, p. 451, Thm. 3.4]. Therefore, if $\mu(z)$ is an eigenvalue of $\mathbf{K^{JAC}}(z)$ and $\lambda(z)$ satisfies (3.10), we can choose

$$\lambda(z) + \tilde{\Omega}(z) - 1 = \sqrt{\lambda(z)}\tilde{\Omega}(z)\mu(z). \tag{3.11}$$

The next lemma determines the optimal (complex) value $\tilde{\Omega}(z)$ which minimizes the spectral radius of $\mathbf{K^{CSOR}}(z)$ for *a given value of z*. The result follows immediately from complex SOR theory, see e.g. [11, Thm. 4.1] or [19, Eq. (9.19)]. The result was rediscovered in [21, Thm. 5.2] and presented in a waveform relaxation context for the $B = I$ case.

LEMMA 3.6. *Assume the matrices B and A are such that $zB + A$ is a block-consistently ordered matrix with nonsingular diagonal blocks. Assume the spectrum $\sigma\left(\mathbf{K^{JAC}}(z)\right)$ lies on a line segment $[-\mu_1(z), \mu_1(z)]$ with $\mu_1(z) \in \mathbb{C} \setminus \{(-\infty, -1] \cup [1, \infty)\}$. The spectral radius of $\mathbf{K^{CSOR}}(z)$ is then minimized for a given value of z by the unique optimum $\tilde{\Omega}_{opt}(z)$, given by*

$$\tilde{\Omega}_{opt}(z) = \frac{2}{1 + \sqrt{1 - \mu_1^2(z)}}, \tag{3.12}$$

where $\sqrt{\cdot}$ denotes the root with the positive real part. In particular,

$$\rho\left(\mathbf{K^{CSOR},opt}(z)\right) = |\tilde{\Omega}_{opt}(z) - 1| < 1. \tag{3.13}$$

Remark 3.2. Following Kredell in [11, Lem. 4.1], the condition on the collinearity of the eigenvalues of the Jacobi symbol can be weakened. For (3.12) to hold, it is sufficient that there exists a *critical eigenvalue pair* $\pm\mu_1(z)$ of $\mathbf{K^{JAC}}(z)$, i.e., for all values of the overrelaxation parameter the pair $\pm\mu_1(z)$ corresponds to the dominant eigenvalue of $\mathbf{K^{CSOR}}(z)$. The existence of such a pair may be difficult to verify in practice, though.

Remark 3.3. The results of the above lemmas rely on the assumption of a block-consistent ordering of the matrix $zB + A$. In the case of semidiscrete parabolic PDEs

in two dimensions, this assumption is, for example, satisfied if B and A correspond to a five-point star and the relaxation is pointwise with lexicographic, diagonal, or red/black ordering of the grid points. It is also satisfied if B and A correspond to a 3×3-stencil—a discretization with linear or bilinear finite elements on a regular triangular or rectangular mesh, for example—and the relaxation is linewise.

Remark 3.4. The assumption that the eigenvalues of the Jacobi symbol are on a line is rather severe. Yet, it is satisfied for certain important classes of problems. For example, this is so when $B = I$ and A is a symmetric positive definite consistently ordered matrix with constant positive diagonal $D_A = d_a I$ ($d_a > 0$). In that case the spectrum of $\mathbf{K^{JAC}}(z)$ equals $d_a/(z + d_a)\sigma(\mathbf{K^{JAC}}(0))$. It is the spectrum of the standard Jacobi iteration matrix, which is real and has maximum smaller than 1 [27, p. 147, Thm. 3.5], scaled and rotated around the origin. If the assumptions of the theorem are violated, a more general complex SOR theory, allowing the eigenvalues of the Jacobi symbol to be in a certain ellipse, should be used, see e.g. [6], [19], [27]. Alternatively, one could decide to continue to use (3.12). Although one gives up optimality then, this practice may lead to a *good enough* convergence, as is illustrated in section 6.

Remark 3.5. If $\mu_1(z) \in \mathbb{C}\backslash\{(-\infty, -1] \cup [1, \infty)\}$ and $\mu_1(z)$ is analytic for $\mathrm{Re}(z) \geq 0$, then $\tilde{\Omega}_{opt}(z)$ is bounded and analytic for $\mathrm{Re}(z) \geq 0$. According to Remark 3.1, Theorem 3.4 may then be applied to calculate the spectral radius of the CSOR operator with optimal kernel $\rho(\mathcal{K}^{CSOR,opt})$. In general, however, $\mu_1(z)$ is known to be only piecewise analytic, with possible discontinuities or lack of smoothness where the maximum switches from one eigenvalue branch to another. In that case, one might opt for using (3.12) with an analytic function $\mu_1(z)$ that approximates the "correct" one at certain values of z (e.g., near the values that correspond to the slowest converging error components).

3.5. Optimal pointwise overrelaxation in the $B = I$ case. In this section, we will study the optimal variants of the three different SOR methods for ODE systems of the form (1.1) with $B = I$. The resulting formulae will be applied to a model problem in section 5.

We first recall the analytical expression of the spectral radius of the SSSOR waveform relaxation operator $\mathcal{K}^{SSSOR}$, as presented by Miekkala and Nevanlinna in [17, Thm. 4.2].

THEOREM 3.7. *Consider* (1.1) *with* $B = I$. *Assume* A *is a consistently ordered matrix with constant positive diagonal* $D_A = d_a I$ ($d_a > 0$), *the eigenvalues of* $\mathbf{K^{JAC}}(0)$ *are real with* $\mu_1 = \rho(\mathbf{K^{JAC}}(0)) < 1$ *and* $0 < \omega < 2$. *Then, if we consider* $\mathcal{K}^{SSSOR}$ *as an operator in* $L_p(0, \infty)$, $1 \leq p \leq \infty$, *we have*

$$\rho(\mathcal{K}^{SSSOR}) = \begin{cases} 1 - \omega + \frac{1}{2}(\omega\mu_1)^2 + (\omega\mu_1)\sqrt{1 - \omega + \frac{1}{4}(\omega\mu_1)^2}, & \omega \leq \omega_d, \\ \dfrac{8(\omega - 1)^2}{8(\omega - 1) - (\omega\mu_1)^2}, & \omega > \omega_d, \end{cases} \tag{3.14}$$

where $\omega_d = (4/3)(2 - \sqrt{4 - 3\mu_1^2})/\mu_1^2$. *Furthermore, we have* $\omega_{opt} = 4/(4 - \mu_1^2) > \omega_d$.

Based on Lemma 3.5 we can derive an analogous expression for the spectral radius of the DSSOR waveform relaxation operator $\mathcal{K}^{DSSOR}$.

THEOREM 3.8. *Consider* (1.1) *with* $B = I$. *Assume* A *is a consistently ordered matrix with constant positive diagonal* $D_A = d_a I$ ($d_a > 0$), *the eigenvalues of* $\mathbf{K^{JAC}}(0)$ *are real with* $\mu_1 = \rho(\mathbf{K^{JAC}}(0)) < 1$ *and* $0 < \omega < 2$. *Then, if we consider* $\mathcal{K}^{DSSOR}$ *as*

an operator in $L_p(0,\infty)$, $1 \le p \le \infty$, *we have*

$$\rho(\mathcal{K}^{DSSOR}) = \begin{cases} 1-\omega+\frac{1}{2}(\omega\mu_1)^2+(\omega\mu_1)\sqrt{1-\omega+\frac{1}{4}(\omega\mu_1)^2}, & \omega \le \omega_d, \\ (\omega-1)\dfrac{1+\frac{1}{4}\frac{\omega\mu_1}{\sqrt{\omega-1}}}{1-\frac{1}{4}\frac{\omega\mu_1}{\sqrt{\omega-1}}}, & \omega > \omega_d, \end{cases} \tag{3.15}$$

where $\omega_d = (4-2\sqrt{4-2\mu_1^2})/\mu_1^2$. *Furthermore, we have that* $\omega_{opt} > \omega_d$.

Proof. Since $B = I$ and $D_A = d_a I$, we have that

$$\sigma(\mathbf{K^{JAC}}(z)) = \frac{d_a}{z+d_a}\sigma(\mathbf{K^{JAC}}(0)). \tag{3.16}$$

In order to apply Lemma 3.5 to the double-splitting case, we note that here $\tilde{\Omega}(z) = \omega$ and that $\lambda(z)$ is an eigenvalue of the DSSOR symbol $\mathbf{K^{DSSOR}}(z)$, which is given by

$$\mathbf{K^{DSSOR}}(z) = \left(z\frac{1}{\omega}I + \left(\frac{1}{\omega}D_A - L_A\right)\right)^{-1} \cdot \left(z\frac{1-\omega}{\omega}I + \left(\frac{1-\omega}{\omega}D_A + U_A\right)\right).$$

With $\mu(0)$ denoting an arbitrary eigenvalue of $\mathbf{K^{JAC}}(0)$, we can rewrite (3.11) as

$$\frac{z}{d_a} = -1 + \frac{\sqrt{\lambda(z)}\omega\mu(0)}{\lambda(z)+\omega-1}.$$

We get equilibrium lines for $|\lambda(z)|$,

$$\frac{z}{d_a} = -1 + \frac{\sqrt{|\lambda(z)|}\omega\mu(0)}{|\lambda(z)|e^{i\frac{t}{2}} + (\omega-1)e^{-i\frac{t}{2}}}, \tag{3.17}$$

by setting $\lambda(z) = |\lambda(z)|e^{it}$ with t varying from 0 to 4π. The supremum of $|\lambda(z)|$ along the imaginary axis is attained at a point where such an equilibrium line osculates the imaginary axis, i.e., when Re $z(t) = 0$ and Re $z'(t) = 0$. In addition, we note that the eigenvalues of $\mathbf{K^{JAC}}(z)$ are collinear, which implies that $\mathbf{K^{JAC}}(z)$ has a critical eigenvalue pair [11, Lem. 4.1]. According to Remark 3.2, the dominant eigenvalue of $\mathbf{K^{DSSOR}}(z)$ is then obtained by replacing $\mu(0)$ by μ_1 in (3.17). This yields for Re $z(t) = 0$ the following condition:

$$4|\lambda(z)|(\omega-1)\cos^2\left(\frac{t}{2}\right) - \sqrt{|\lambda(z)|}\omega\mu_1(|\lambda(z)|+\omega-1)\cos\left(\frac{t}{2}\right) + (|\lambda(z)|-\omega+1)^2 = 0, \tag{3.18}$$

while Re $z'(t) = 0$ gives

$$\left(4|\lambda(z)|(\omega-1)\cos\left(\frac{t}{2}\right) - \frac{1}{2}\sqrt{|\lambda(z)|}\omega\mu_1(|\lambda(z)|+\omega-1)\right)\sin\left(\frac{t}{2}\right) = 0. \tag{3.19}$$

If $\sin(t/2) = 0$, the osculation with the imaginary axis occurs at the origin and the corresponding largest value of $|\lambda(0)|$ equals the spectral radius of the algebraic SOR method [25], [27], which, for $\omega \le \omega_{opt}^{alg} = 2/(1+\sqrt{1-\mu_1^2})$, is given by

$$|\lambda(0)| = 1-\omega+\frac{1}{2}(\omega\mu_1)^2+(\omega\mu_1)\sqrt{1-\omega+\frac{1}{4}(\omega\mu_1)^2}. \tag{3.20}$$

If $\sin(t/2) \neq 0$, the osculation is at a complex point $z = i\xi$, $\xi \neq 0$ (and by symmetry at $z = -i\xi$). The corresponding value of $|\lambda(z)|$ is obtained by eliminating $\cos(t/2)$ from (3.18) and (3.19). This gives the equation

$$|\lambda(z)|^2 + \left(\frac{-32(\omega-1)^2 - 2\omega^2(\omega-1)\mu_1^2}{16(\omega-1) - \omega^2\mu_1^2} \right) |\lambda(z)| + (\omega-1)^2 = 0,$$

whose largest solution for $\omega > 1$ equals

$$|\lambda(z)| = (\omega-1) \frac{1 + \frac{1}{4}\frac{\omega\mu_1}{\sqrt{\omega-1}}}{1 - \frac{1}{4}\frac{\omega\mu_1}{\sqrt{\omega-1}}}. \tag{3.21}$$

In order to determine the range of validity of this result, we need in (3.19) to specify the condition that $-1 < \cos(t/2) < 1$. This is a condition on ω which, when combined with (3.21), leads to $\omega > \omega_d$ with ω_d as given in the formulation of the theorem. It turns out that $1 < \omega_d < \omega_{opt}^{alg}$ and that (3.21) is larger than (3.20) for $\omega_d < \omega \leq \omega_{opt}^{alg}$. Hence, the proof is completed by combining the latter two expressions. ∎

Finally, we investigate the spectral radius of $\mathcal{K}^{CSOR,opt}$, the convolution SOR waveform operator with optimal kernel.

THEOREM 3.9. *Consider* (1.1) *with* $B = I$. *Assume* A *is a consistently ordered matrix with constant positive diagonal* $D_A = d_a I$ $(d_a > 0)$ *and the eigenvalues of* $\mathbf{K^{JAC}}(0)$ *are real with* $\mu_1 = \rho(\mathbf{K^{JAC}}(0)) < 1$. *Then, if we consider* $\mathcal{K}^{CSOR,opt}$ *as an operator in* $L_p(0,\infty)$, $1 \leq p \leq \infty$, *we have*

$$\rho(\mathcal{K}^{CSOR,opt}) = \frac{\mu_1^2}{(1 + \sqrt{1-\mu_1^2})^2}. \tag{3.22}$$

Proof. Under the assumptions of the theorem we have (3.16). Hence, we may apply Lemma 3.6 with

$$\mu_1(z) = \frac{d_a}{z + d_a}\mu_1$$

in order to derive the optimum complex overrelaxation parameter $\tilde{\Omega}_{opt}(z)$. Since $\tilde{\Omega}_{opt}(z)$ is a bounded analytic function in the complex right-half plane, including the imaginary axis, we know from Remark 3.1 that it is the Laplace transform of a function of the form (2.6), with $\omega_c(t)$ in $L_1(0,\infty)$. Thus, we may apply Theorem 3.4, which, when combined with (3.13), yields

$$\rho(\mathcal{K}^{CSOR,opt}) = \sup_{\xi\in\mathbb{R}} \rho(\mathbf{K^{CSOR},}^{opt}(i\xi)) = \sup_{\xi\in\mathbb{R}} |\tilde{\Omega}_{opt}(i\xi) - 1| = \sup_{\xi\in\mathbb{R}} \frac{|\mu_1(i\xi)|^2}{|1 + \sqrt{1-\mu_1^2(i\xi)}|^2}.$$

Since the numerator is maximal for $\xi = 0$, and the denominator is minimal for $\xi = 0$, the latter supremum is obtained for $\xi = 0$. This completes the proof. ∎

Since the maximum of $\rho(\mathbf{K^{CSOR},}^{opt}(z))$ is found at the complex origin, we can easily state and prove the following properties.

PROPERTY 3.1. *Under the assumptions of Theorem* 3.9, *pointwise optimal convolution SOR waveform relaxation for the ODE system* $\dot{u} + Au = f$ *attains the same asymptotic convergence rate as optimal algebraic SOR for the linear system* $Au = f$.

Proof. This follows from $\tilde{\Omega}_{opt}(0) = \omega_{opt}^{alg}$. ∎

TABLE 3.1
Spectral radii of optimal SSSOR, DSSOR, and CSOR waveform relaxation for problem (1.1) *with* $B = I$ *and* $D_A = d_a I$. *The value of the optimal parameter* ω_{opt} *is given in parenthesis.*

μ_1	0.9	0.95	0.975	0.9875
$\rho(\mathcal{K}^{SSSOR,\omega_{opt}})$	0.681 (1.2539)	0.822 (1.2913)	0.906 (1.3117)	0.952 (1.3224)
$\rho(\mathcal{K}^{DSSOR,\omega_{opt}})$	0.750 (1.1374)	0.867 (1.1539)	0.932 (1.1626)	0.965 (1.1671)
$\rho(\mathcal{K}^{CSOR,opt})$	0.393	0.524	0.636	0.728

PROPERTY 3.2. *Under the assumptions of Theorem* 3.9, *we have that* $\Omega_{opt}(t) = \delta(t) + (\omega_c)_{opt}(t)$. *Also* ω_{opt}^{alg}, *the optimal overrelaxation parameter for the system* $Au = f$ *satisfies* $\omega_{opt}^{alg} = 1 + \int_0^\infty (\omega_c)_{opt}(t)dt$.

Proof. We have that $\lim_{z->\infty} \mu_1(z) = 0$. Hence, $\lim_{z->\infty} \tilde{\Omega}_{opt}(z) = 1$ and the first result follows. The second result follows from $\tilde{\Omega}_{opt}(0) = \omega_{opt}^{alg}$ and the definition of the Laplace transform. ∎

PROPERTY 3.3. *Under the assumptions of Theorem* 3.9, *we have that* $\mathcal{K}^{CSOR,opt}$ *is a convolution operator.*

Proof. The matrix multiplication part of $\mathcal{K}^{CSOR,opt}$ satisfies

$$K^{CSOR,opt} = \lim_{z->\infty} \mathbf{K}^{\mathbf{CSOR},opt}(z) = 0.$$

Hence, by Theorem 3.2, $\mathcal{K}^{CSOR,opt}$ is a convolution operator with an L_1-kernel. ∎

Using formulae (3.14), (3.15), and (3.22), we can compute the spectral radii of the optimal SSSOR, DSSOR, and CSOR waveform relaxation methods as a function of μ_1. These values are presented in Table 3.1, together with the values of the optimal parameter ω_{opt} for the SSSOR and DSSOR method.

4. Discrete-time convergence analysis. In this section we will analyze the discrete-time SOR waveform relaxation methods outlined in section 2.2, following the theoretical framework developed in [9]. We will identify the nature and the convergence properties of the discrete-time CSOR iteration operator. The results for the discrete-time standard SOR waveform method are then obtained by setting $\omega_c[n] \equiv 0$. The corresponding results for the SOR method with single splitting can be found in [18].

4.1. Nature of the operator. Since we do not iterate on the k starting values, we use a shifted subscript τ-notation for sequences u_τ of which the initial values $u[n]$, $n < k$ are known, i.e., $u_\tau = \{u[k+n]\}_{n=0}^{N-1}$. The discrete-time version of Lemma 3.1 reads as follows.

LEMMA 4.1. *The solution to the difference equation*

$$\sum_{l=0}^{k} \left(\frac{1}{\tau} \alpha_l b + \beta_l a \right) u[n+l] = \sum_{l=0}^{k} \left(\frac{1}{\tau} \alpha_l q + \beta_l p \right) v[n+l] + \sum_{l=0}^{k} \beta_l w[n+l], \quad n \geq 0,$$

with $b, a, q, p \in \mathbb{C}^{m \times m}$ *and* b *nonsingular is given by* $u_\tau = \mathcal{K}_\tau v_\tau + \varphi_\tau$, *with* $\mathcal{K}_\tau$ *a discrete convolution operator:*

$$(\mathcal{K}_\tau x_\tau)[n] = (k_\tau \star x_\tau)[n] = \sum_{l=0}^{n} k[n-l]x[l], \quad n \geq 0,$$

and φ_τ depending on $w[l]$, $l \geq 0$, and the initial values $u[l]$, $v[l]$, $l = 0, \ldots, k-1$. The sequence $k_\tau \in l_1(\infty)$ if $\sigma(-\tau b^{-1}a) \subset \operatorname{int} S$, where S is the stability region of the linear multistep method. If, in addition, $w_\tau \in l_p(\infty)$, then $\varphi_\tau \in l_p(\infty)$.

Proof. The proof of the lemma is based on a Z-transform argument and the use of Wiener's inversion theorem for discrete l_1-sequences. It is analogous to the proof of [9, Lem. 4.3]. ∎

The discrete-time CSOR scheme can be written as a classical successive approximation method, $u_\tau^{(\nu)} = \mathcal{K}_\tau^{CSOR} u_\tau^{(\nu-1)} + \varphi_\tau$. Here, φ_τ is a sequence which depends on the difference equation's right-hand side f_τ and the initial conditions, while the nature of the discrete-time CSOR operator $\mathcal{K}_\tau^{CSOR}$ is identified below.

THEOREM 4.2. *The discrete-time CSOR waveform relaxation operator $\mathcal{K}_\tau^{CSOR}$ is a discrete convolution operator, whose matrix-valued kernel $k_\tau^{CSOR} \in l_1(\infty)$ if $\sigma(-\tau D_B^{-1} D_A) \subset \operatorname{int} S$ and $\Omega_\tau \in l_1(\infty)$.*

Proof. Discretization of (2.1) and (2.5) leads to the discrete-time CSOR scheme, given by

$$\begin{aligned}\sum_{l=0}^{k} \left(\frac{1}{\tau}\alpha_l b_{ii} + \beta_l a_{ii}\right) \hat{u}_i^{(\nu)}[n+l] &= -\sum_{j=1}^{i-1}\sum_{l=0}^{k} \left(\frac{1}{\tau}\alpha_l b_{ij} + \beta_l a_{ij}\right) u_j^{(\nu)}[n+l] \\ &\quad - \sum_{j=i+1}^{d_b}\sum_{l=0}^{k} \left(\frac{1}{\tau}\alpha_l b_{ij} + \beta_l a_{ij}\right) u_j^{(\nu-1)}[n+l] + \sum_{l=0}^{k} \beta_l f_i[n+l], \quad n \geq 0,\end{aligned} \tag{4.1}$$

and (2.8).

Application of Lemma 4.1 to (4.1) gives

$$(\hat{u}_i^{(\nu)})_\tau = \sum_{j=1}^{i-1} (h_{ij})_\tau \star (u_j^{(\nu)})_\tau + \sum_{j=i+1}^{d_b} (h_{ij})_\tau \star (u_j^{(\nu-1)})_\tau + (\phi_i)_\tau, \tag{4.2}$$

with $(h_{ij})_\tau \in l_1(\infty)$ if $\sigma(-\tau\, b_{ii}^{-1} a_{ii}) \subset \operatorname{int} S$ and $(\phi_i)_\tau$ an $l_p(\infty)$-sequence.

It is now easy to prove that there exist l_1-sequences $(k_{ij}^{CSOR})_\tau$ such that

$$(u_i^{(\nu)})_\tau = \sum_{j=1}^{d_b} (k_{ij}^{CSOR})_\tau \star (u_j^{(\nu-1)})_\tau + (\varphi_i)_\tau. \tag{4.3}$$

Indeed, the combination of (4.2) and (2.8) for $i = 1$ gives $(k_{11}^{CSOR})_\tau = (\delta_\tau - \Omega_\tau)I$, $(k_{1j}^{CSOR})_\tau = \Omega_\tau \star (h_{1j})_\tau$, $2 \leq j \leq d_b$, and $(\varphi_1)_\tau = (\Omega_\tau \star (\phi_1)_\tau)I$ with I the identity matrix of the appropriate dimension in the case of block relaxation.

The general case involves the computation of $(u_i^{(\nu)})_\tau$ from (4.2) and (2.8). It follows by induction on i and is based on the elimination of the sequences $(u_j^{(\nu)})_\tau$, $j < i$, from (4.2) using (4.3). Consequently, the resulting $(k_{ij}^{CSOR})_\tau$, which consist of linear combinations and convolutions of l_1-sequences, belong to $l_1(\infty)$. ∎

4.2. Symbol. Discrete Laplace or Z-transformation of the iterative scheme of the discrete-time CSOR waveform relaxation method yields an iteration of the form $\tilde{u}_\tau^{(\nu)}(z) = \mathbf{K}_\tau^{\mathbf{CSOR}}(z)\tilde{u}_\tau^{(\nu-1)}(z) + \tilde{\varphi}_\tau(z)$ with $\tilde{u}_\tau^{(\nu)}(z) = \mathcal{Z}\left(u_\tau^{(\nu)}\right) = \sum_{i=0}^{\infty} u^{(\nu)}[i] z^{-i}$ and

$\mathbf{K}_\tau^{\mathbf{CSOR}}(z)$ the discrete-time CSOR symbol. This symbol is given by

$$\mathbf{K}_\tau^{\mathbf{CSOR}}(z) = \left(\frac{1}{\tau}\frac{a}{b}(z)\left(\frac{1}{\tilde{\Omega}_\tau(z)}D_B - L_B\right) + \left(\frac{1}{\tilde{\Omega}_\tau(z)}D_A - L_A\right)\right)^{-1} \cdot \left(\frac{1}{\tau}\frac{a}{b}(z)\left(\frac{1-\tilde{\Omega}_\tau(z)}{\tilde{\Omega}_\tau(z)}D_B + U_B\right) + \left(\frac{1-\tilde{\Omega}_\tau(z)}{\tilde{\Omega}_\tau(z)}D_A + U_A\right)\right),$$

with $\tilde{\Omega}_\tau(z) = \omega + (\tilde{\omega}_c)_\tau(z)$.

4.3. Spectral radii and norm. The theorems in this section follow immediately from the general theory in [9, section 2], where we analyzed the properties of discrete convolution operators. For the iteration on finite intervals we have the following result from [9, Lem. 2.1].

THEOREM 4.3. *Assume that the discrete solvability condition* (2.9) *is satisfied, and consider the discrete-time CSOR operator* $\mathcal{K}_\tau^{CSOR}$ *as an operator in* $l_p(N)$ *with* $1 \le p \le \infty$ *and* N *finite. Then,* $\mathcal{K}_\tau^{CSOR}$ *is a bounded operator and*

$$\rho(\mathcal{K}_\tau^{CSOR}) = \rho(\mathbf{K}_\tau^{\mathbf{CSOR}}(\infty)). \tag{4.4}$$

If $\sigma(-\tau D_B^{-1}D_A) \subset \text{int } S$, Theorem 4.2 implies that the kernel of the CSOR operator belongs to $l_1(\infty)$. Hence, we may apply [9, Lems. 2.2 and 2.3] in order to derive the following infinite-interval result.

THEOREM 4.4. *Assume* $\sigma(-\tau D_B^{-1}D_A) \subset \text{int } S$ *and* $\Omega_\tau \in l_1(\infty)$. *Consider the discrete-time CSOR iteration operator* $\mathcal{K}_\tau^{CSOR}$ *as an operator in* $l_p(\infty)$, $1 \le p \le \infty$. *Then,* $\mathcal{K}_\tau^{CSOR}$ *is a bounded operator and*

$$\rho(\mathcal{K}_\tau^{CSOR}) = \max_{|z|\ge 1} \rho(\mathbf{K}_\tau^{\mathbf{CSOR}}(z)) = \max_{|z|=1} \rho(\mathbf{K}_\tau^{\mathbf{CSOR}}(z)). \tag{4.5}$$

If we denote by $||\cdot||_2$ *the* l_2*-norm and by* $||\cdot||$ *the Euclidean vector norm, we have*

$$||\mathcal{K}_\tau^{CSOR}||_2 = \max_{|z|\ge 1} ||\mathbf{K}_\tau^{\mathbf{CSOR}}(z)|| = \max_{|z|=1} ||\mathbf{K}_\tau^{\mathbf{CSOR}}(z)||. \tag{4.6}$$

Remark 4.1. In Theorem 4.4, we require $\tilde{\Omega}_\tau(z)$ to be the Z-transform of an l_1-kernel Ω_τ. For this, a sufficient (but not necessary) condition is that $\tilde{\Omega}_\tau(z)$ is a bounded and analytic function in an open domain containing $\{z \in \mathbb{C} \mid |z| \ge 1\}$. A tighter set of conditions can be found in [5, p. 71].

The following lemma is the discrete-time equivalent of Lemma 3.6. It involves the eigenvalue distribution of the discrete-time Jacobi symbol, which is related to its continuous-time equivalent by [9, Eq. (4.10)],

$$\mathbf{K}_\tau^{\mathbf{JAC}}(z) = \mathbf{K}^{\mathbf{JAC}}\left(\frac{1}{\tau}\frac{a}{b}(z)\right). \tag{4.7}$$

LEMMA 4.5. *Assume the matrices* B *and* A *are such that* $\frac{1}{\tau}\frac{a}{b}(z)B + A$ *is a block-consistently ordered matrix with nonsingular diagonal blocks. Assume the spectrum* $\sigma\left(\mathbf{K}_\tau^{\mathbf{JAC}}(z)\right)$ *lies on a line segment* $[-(\mu_1)_\tau(z), (\mu_1)_\tau(z)]$ *with* $(\mu_1)_\tau(z) \in \mathbb{C} \setminus \{(-\infty,-1] \cup [1,\infty)\}$. *The spectral radius of* $\mathbf{K}_\tau^{\mathbf{CSOR}}(z)$ *is then minimized for a given value of* z *by the unique optimum* $(\tilde{\Omega}_{opt})_\tau(z)$, *given by*

$$(\tilde{\Omega}_{opt})_\tau(z) = \frac{2}{1 + \sqrt{1 - (\mu_1)_\tau^2(z)}}, \tag{4.8}$$

where $\sqrt{\cdot}$ denotes the root with the positive real part. In particular,

$$\rho(\mathbf{K}_\tau^{\mathbf{CSOR},opt}(z)) = |(\tilde{\Omega}_{opt})_\tau(z) - 1| < 1. \tag{4.9}$$

Proof. In analogy with Lemma 3.6, the result follows from standard complex SOR theory applied to the complex matrix $\frac{1}{\tau}\frac{a}{b}(z)B + A$. ∎

4.4. Continuous-time versus discrete-time results. Under the assumption

$$\tilde{\Omega}_\tau(z) = \tilde{\Omega}\left(\frac{1}{\tau}\frac{a}{b}(z)\right), \tag{4.10}$$

the discrete-time and continuous-time CSOR symbols are related by a formula similar to (4.7), i.e.,

$$\mathbf{K}_\tau^{\mathbf{CSOR}}(z) = \mathbf{K}^{\mathbf{CSOR}}\left(\frac{1}{\tau}\frac{a}{b}(z)\right).$$

As a result, we have the following two theorems which provide the spectral radius of the discrete-time operator in terms of the symbol of the continuous-time operator. They correspond to Theorems 4.1 and 4.4 in [9], so we can omit their proofs.

THEOREM 4.6. *Assume that both* (4.10) *and the discrete solvability condition* (2.9) *are satisfied, and consider $\mathcal{K}_\tau^{CSOR}$ as an operator in $l_p(N)$ with $1 \le p \le \infty$ and N finite. Then,*

$$\rho(\mathcal{K}_\tau^{CSOR}) = \rho\left(\mathbf{K}^{\mathbf{CSOR}}\left(\frac{1}{\tau}\frac{\alpha_k}{\beta_k}\right)\right). \tag{4.11}$$

THEOREM 4.7. *Assume* (4.10) *and $\sigma(-\tau D_B^{-1}D_A) \subset \operatorname{int} S$, and consider $\mathcal{K}_\tau^{CSOR}$ as an operator in $l_p(\infty)$, $1 \le p \le \infty$. Then,*

$$\rho(\mathcal{K}_\tau^{CSOR}) = \sup\{\rho(\mathbf{K}^{\mathbf{CSOR}}(z)) \mid \tau z \in \mathbb{C} \setminus \operatorname{int} S\} = \sup_{\tau z \in \partial S} \rho(\mathbf{K}^{\mathbf{CSOR}}(z)). \tag{4.12}$$

Also, in complete analogy to the result in [9, sect. 4.3], (4.10) implies that

$$\lim_{\tau \to 0} \rho\left(\mathcal{K}_\tau^{CSOR}\right) = \rho\left(\mathcal{K}^{CSOR}\right), \tag{4.13}$$

for both the finite and infinite time-interval computation.

Observe that equality (4.10), and, hence, Theorems 4.6 and 4.7 and equality (4.13), are not necessarily satisfied. They do hold, however, in the two important cases explained below.

The first case concerns the standard SOR waveform method with double splitting. Indeed, if $\omega_c(t) \equiv 0$ and $\omega_c[n] \equiv 0$, we have $\tilde{\Omega}_\tau(z) \equiv \tilde{\Omega}\left(\frac{1}{\tau}\frac{a}{b}(z)\right) \equiv \omega$.

Equality (4.10) is also satisfied for the optimal CSOR method. As the discrete-time and continuous-time Jacobi symbols are related by (4.7), a similar relation holds for their respective eigenvalues with largest modulus: $(\mu_1)_\tau(z) = \mu_1\left(\frac{1}{\tau}\frac{a}{b}(z)\right)$. Hence, by comparing the formulae for the optimal convolution kernels in Lemmas 3.6 and 4.5, we find

$$(\tilde{\Omega}_{opt})_\tau(z) = \tilde{\Omega}_{opt}\left(\frac{1}{\tau}\frac{a}{b}(z)\right).$$

5. Pointwise SOR waveform relaxation: Model problem analysis and numerical results. We consider the m-dimensional heat equation

$$\frac{\partial \mathbf{u}}{\partial t} - \Delta_m \mathbf{u} = 0, \quad x \in [0,1]^m, \quad t > 0, \tag{5.1}$$

with Dirichlet boundary conditions and a given initial condition. We discretize using finite differences or finite elements on a regular grid with mesh-size h.

5.1. Finite-difference discretization. A finite-difference discretization of (5.1) with central differences leads to a system of ODEs of the form (1.1) with mass matrix $B = I$ and stiffness matrix A, which, in the one-dimensional and two-dimensional case, is given, respectively, by the stencils

$$A = \frac{1}{h^2}\,[-1 \;\; 2 \;\; -1] \quad \text{and} \quad A = \frac{1}{h^2}\begin{bmatrix} & -1 & \\ -1 & 4 & -1 \\ & -1 & \end{bmatrix}.$$

Matrix A is consistently ordered for an iteration with pointwise relaxation in a lexicographic, red/black or diagonal ordering. The eigenvalues of the Jacobi iteration matrix corresponding to matrix A are well known. They are real and one has independent of the spatial dimension that

$$\mu_1 = \rho(\mathbf{K}^{\mathbf{JAC}}(0)) = \cos(\pi h). \tag{5.2}$$

Hence, the assumptions of Theorems 3.7, 3.8, and 3.9 are satisfied. In Figure 5.1, we illustrate formulae (3.14) and (3.15) by depicting the spectral radii of the single- and double-splitting operators $\rho(\mathcal{K}^{SSSOR})$ and $\rho(\mathcal{K}^{DSSOR})$, together with $\rho(\mathcal{K}^{SOR}_{alg})$, the spectral radius of the standard SOR iteration matrix for the linear system $Au = f$, as a function of ω.

In [17, p. 473], Miekkala and Nevanlinna derived the following result for the optimal single-splitting SOR waveform method from Theorem 3.7.

PROPERTY 5.1. *Consider model problem* (5.1)*, discretized with finite differences. Then, if we consider* $\mathcal{K}^{SSSOR,\omega_{opt}}$ *as an operator in* $L_p(0,\infty)$*,* $1 \le p \le \infty$*, we have for small* h *that*

$$\rho(\mathcal{K}^{SSSOR,\omega_{opt}}) \approx 1 - 2\pi^2 h^2, \quad \omega_{opt} \approx \frac{4}{3} - \frac{4}{9}\pi^2 h^2. \tag{5.3}$$

A similar result can be proven for the optimal DSSOR waveform relaxation method. The calculation is standard, but rather lengthy and tedious. It was performed by using the formula manipulator Mathematica [26]. The computation is based on first differentiating (3.15) with respect to ω and then finding the zeros of the resulting expression. The formula for ω_{opt} is then substituted back into (3.15). Finally, entering (5.2) and calculating a series expression for small h leads to the desired result.

PROPERTY 5.2. *Consider model problem* (5.1)*, discretized with finite differences. Then, if we consider* $\mathcal{K}^{DSSOR,\omega_{opt}}$ *as an operator in* $L_p(0,\infty)$*,* $1 \le p \le \infty$*, we have for small* h *that*

$$\rho(\mathcal{K}^{DSSOR,\omega_{opt}}) \approx 1 - \sqrt{2}\,\pi^2 h^2, \quad \omega_{opt} \approx (4 - 2\sqrt{2}) + \left(3 - \frac{9\sqrt{2}}{4}\right)\pi^2 h^2. \tag{5.4}$$

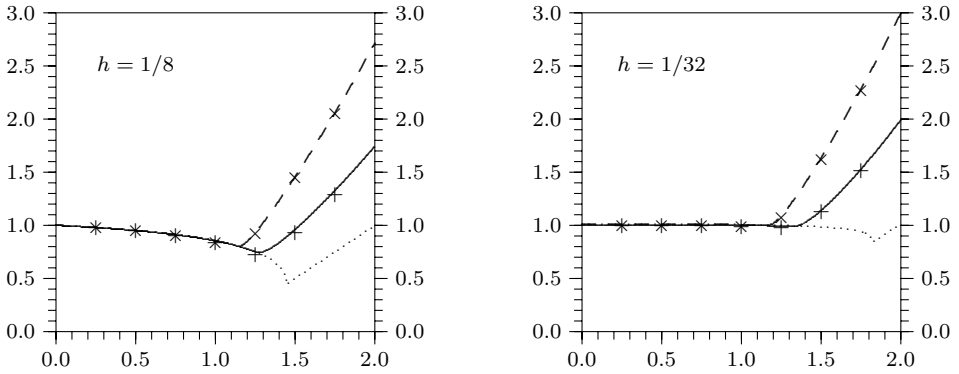

FIG. 5.1. *$\rho(\mathcal{K}^{SSSOR})$ (solid), $\rho(\mathcal{K}^{DSSOR})$ (dashed) and $\rho(\mathcal{K}_{alg}^{SOR})$ (dots) vs. ω for model problem* (5.1) *with finite-difference discretization. The "+"- and "×"-symbols indicate measured values from numerical experiments (section* 5.4*).*

TABLE 5.1
Spectral radii of optimal SSSOR, DSSOR, and CSOR waveform relaxation for model problem (5.1) *with finite-difference discretization. The value of the optimal parameter ω_{opt} is given in parenthesis.*

h	1/8	1/16	1/32	1/64
$\rho(\mathcal{K}^{SSSOR,\omega_{opt}})$	0.745 (1.2713)	0.927 (1.3166)	0.981 (1.3291)	0.995 (1.3323)
$\rho(\mathcal{K}^{DSSOR,\omega_{opt}})$	0.804 (1.1452)	0.947 (1.1647)	0.986 (1.1698)	0.997 (1.1711)
$\rho(\mathcal{K}^{CSOR,opt})$	0.446	0.674	0.821	0.906

For the CSOR waveform relaxation method with optimal overrelaxation kernel we may invoke Property 3.1. The operator's spectral radius equals that of the optimal SOR iteration matrix for the discrete Laplace operator.

PROPERTY 5.3. *Consider model problem* (5.1)*, discretized with finite differences. Then, if we consider $\mathcal{K}^{CSOR,opt}$ as an operator in $L_p(0,\infty)$, $1 \le p \le \infty$, we have for small h that*

$$\rho(\mathcal{K}^{CSOR,opt}) \approx 1 - 2\,\pi\,h. \tag{5.5}$$

Numerical values of these spectral radii, together with the corresponding ω_{opt} are presented in Table 5.1 as a function of the mesh-size h. They are computed from (3.14), (3.15), and (3.22).

5.2. Finite-element discretization. A finite-element discretization of (5.1) does not in general lead to a matrix $zB + A$ that is consistently ordered for point relaxation. This precludes the use of Lemma 3.5. An exception is the one-dimensional model problem (5.1) discretized with linear finite elements. In that case one obtains a system of ODEs of the form (1.1) where B and A are given by the stencils

$$B = \frac{h}{6}\,[\ 1\ \ 4\ \ 1\ ] \quad \text{and} \quad A = \frac{1}{h}\,[\ -1\ \ 2\ \ -1\ ]. \tag{5.6}$$

In the following theorem, we derive the spectral radius of the DSSOR waveform relaxation operator, based on the DSSOR versions of Theorem 3.4 and Lemma 3.5. In particular, we set $\tilde{\Omega}(z) = \omega$ so that the right-hand side of (3.4) becomes $\mathbf{K}^{\mathbf{DSSOR}}(z)$.

THEOREM 5.1. *Consider* (1.1) *with* B *and* A *given by* (5.6). *Assume* $0 < \omega < 2$. *Then, if we consider* $\mathcal{K}^{DSSOR}$ *as an operator in* $L_p(0,\infty)$, $1 \le p \le \infty$, *we have with* $\mu_1 = \cos(\pi h)$ *that*

$$\rho(\mathcal{K}^{DSSOR}) = \begin{cases} 1-\omega+\frac{1}{2}(\omega\mu_1)^2+\omega\mu_1\sqrt{1-\omega+\frac{1}{4}(\omega\mu_1)^2}, & \omega \le \omega_d, \\ (\omega-1)\dfrac{1+\frac{3}{8}\frac{\omega\mu_1}{\sqrt{\omega-1+\frac{1}{8}\omega^2\mu_1^2}}}{1-\frac{3}{8}\frac{\omega\mu_1}{\sqrt{\omega-1+\frac{1}{8}\omega^2\mu_1^2}}}, & \omega > \omega_d, \end{cases} \tag{5.7}$$

with $\omega_d = (8-4\sqrt{4-\mu_1^2})/\mu_1^2$. *Furthermore, we have* $\omega_{opt} > \omega_d$.

Proof. The spectrum of the Jacobi symbol is given by

$$\sigma(\mathbf{K^{JAC}}(z)) = \left\{ \frac{-2zh^2+12}{4zh^2+12}\ \mu_j \;\middle|\; 1 \le j \le \frac{1}{h}-1 \right\} \quad \text{with} \quad \mu_j = \cos(j\pi h). \tag{5.8}$$

Since the conditions of Lemma 3.5 are satisfied, (3.11) can be written as

$$\lambda(z)+\omega-1 = \sqrt{\lambda(z)}\omega\frac{-2zh^2+12}{4zh^2+12}\mu_j,$$

or, after setting $\lambda(z) = |\lambda(z)|e^{it}$,

$$z = \frac{-3}{h^2}\frac{|\lambda(z)|e^{i\frac{t}{2}}+(\omega-1)e^{-i\frac{t}{2}}-\sqrt{|\lambda(z)|}\omega\mu_j}{|\lambda(z)|e^{i\frac{t}{2}}+(\omega-1)e^{-i\frac{t}{2}}+\frac{1}{2}\sqrt{|\lambda(z)|}\omega\mu_j}. \tag{5.9}$$

In complete analogy with the proof of Theorem 3.8, we replace μ_j by μ_1 and impose the conditions Re $z(t) = 0$ and Re $z'(t) = 0$ on the equilibrium curve (5.9) to determine the supremum of $|\lambda(z)|$ along the imaginary axis. This gives

$$\begin{aligned} &4|\lambda(z)|(\omega-1)\cos^2\left(\frac{t}{2}\right)-\frac{1}{2}\sqrt{|\lambda(z)|}\omega\mu_j(|\lambda(z)|+\omega-1)\cos\left(\frac{t}{2}\right) \\ &+(|\lambda(z)|+\omega-1)^2-\frac{1}{2}|\lambda(z)|\omega^2\mu_j^2 = 0 \end{aligned}$$

and

$$\left(4|\lambda(z)|(\omega-1)\cos\left(\frac{t}{2}\right)-\frac{1}{4}\sqrt{|\lambda(z)|}\omega\mu_j(|\lambda(z)|+\omega-1)\right)\sin\left(\frac{t}{2}\right) = 0.$$

We deduce that either the supremum is attained at the origin giving (3.20), or the supremum is found at a certain point $z = i\xi$ ($\xi \neq 0$) giving

$$|\lambda(z)| \;=\; (\omega-1)\frac{1+\frac{3}{8}\frac{\omega\mu_1}{\sqrt{\omega-1+\frac{1}{8}\omega^2\mu_1^2}}}{1-\frac{3}{8}\frac{\omega\mu_1}{\sqrt{\omega-1+\frac{1}{8}\omega^2\mu_1^2}}}. \tag{5.10}$$

The proof is completed by combining (3.20) and (5.10). The value of ω_d is derived by determining the least value of ω for which the supremum is not attained at the origin. It turns out that $1 < \omega_d < \omega_{opt}^{alg}$. ∎

Equation (5.7) is illustrated in Figure 5.2, where the theoretical values of the spectral radius are plotted against ω.

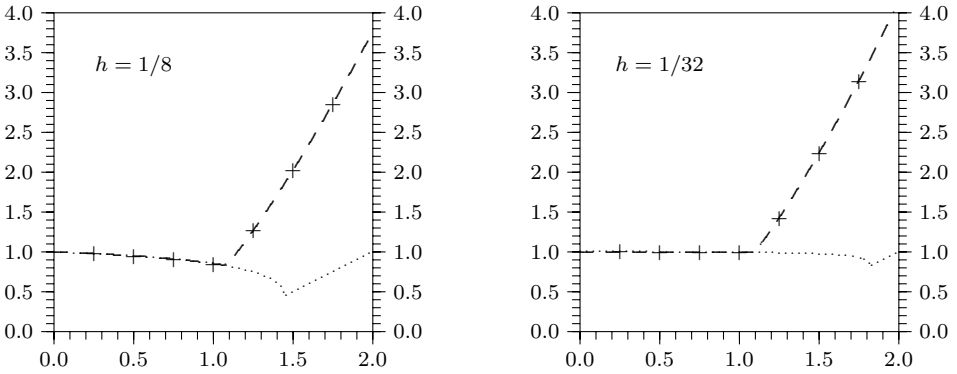

FIG. 5.2. $\rho(\mathcal{K}^{DSSOR})$ *(dashed) and* $\rho(\mathcal{K}^{SOR}_{alg})$ *(dots) vs.* ω *for model problem* (5.1) *with* $m = 1$ *and linear finite-element discretization. The "+"-symbols indicate measured values from numerical experiments (section* 5.4*).*

TABLE 5.2
Parameters ω_d *and* ω_{opt}*, together with spectral radii of optimal DSSOR and CSOR waveform relaxation for model problem* (5.1) *with* $m = 1$ *and linear finite-element discretization.*

h	1/8	1/16	1/32	1/64
ω_d	1.0599	1.0687	1.0710	1.0716
ω_{opt}	1.0625	1.0694	1.0712	1.0716
$\rho(\mathcal{K}^{DSSOR,\omega_{opt}})$	0.834	0.956	0.989	0.997
$\rho(\mathcal{K}^{CSOR,opt})$	0.446	0.674	0.821	0.906

The spectral radius of the CSOR waveform relaxation operator with optimal kernel is calculated in the following theorem. As in the finite-difference case, it equals the spectral radius of the optimal standard SOR method for the system $Au = f$ where A is the discrete Laplacian.

THEOREM 5.2. *Consider* (1.1) *with* B *and* A *given by* (5.6)*. Then, if we consider* $\mathcal{K}^{CSOR,opt}$ *as an operator in* $L_p(0,\infty)$*,* $1 \le p \le \infty$*, we have for small* h *that*

$$\rho(\mathcal{K}^{CSOR,opt}) \approx 1 - 2\pi h. \tag{5.11}$$

Proof. Because of (5.8), we have that the eigenvalues of $\mathbf{K}^{\mathbf{JAC}}(z)$ lie on the line segment $[-\mu_1(z), \mu_1(z)]$ with $|\mu_1(z)| < 1$. Therefore, the conditions of Lemma 3.6 are satisfied. Since $\mu_1(z)$ is an analytic function for $\mathrm{Re}(z) \ge 0$, so is $\tilde{\Omega}_{opt}(z)$. Hence, we may apply Theorem 3.4 and Lemma 3.6 to find

$$\rho(\mathcal{K}^{CSOR,opt}) = \sup_{\xi\in\mathbb{R}} |\tilde{\Omega}_{opt}(i\xi) - 1| = |\tilde{\Omega}_{opt}(0) - 1|,$$

from which the result follows. ∎

Table 5.2 shows some values of ω_d, ω_{opt} and $\rho(\mathcal{K}^{DSSOR,\omega_{opt}})$ calculated by means of (5.7). The latter spectral radii obviously satisfy a relation of the form $1 - O(h^2)$. For comparison purposes we have also added the spectral radii of optimal convolution SOR waveform relaxation, which are identical to the ones in Table 5.1.

5.3. Effect of time discretization. We analyze the use of the Crank–Nicolson (CN) method and the backward differentiation (BDF) formulae of order 1 up to 5, for the one-dimensional model problem (5.1) with linear finite-element discretization on a

TABLE 5.3
Spectral radii of discrete-time optimal DSSOR and CSOR waveform relaxation for model problem (5.1) *with* $m = 1$ *and linear finite-element discretization* ($h = 1/16$, $\tau = 1/100$).

multistep method	CN	BDF(1)	BDF(2)	BDF(3)	BDF(4)	BDF(5)
$\rho(\mathcal{K}_\tau^{DSSOR,\omega^\star})$	0.956	0.956	0.956	0.991	1.236	2.113
$\rho(\mathcal{K}_\tau^{CSOR,opt})$	0.674	0.674	0.674	0.674	0.674	0.674

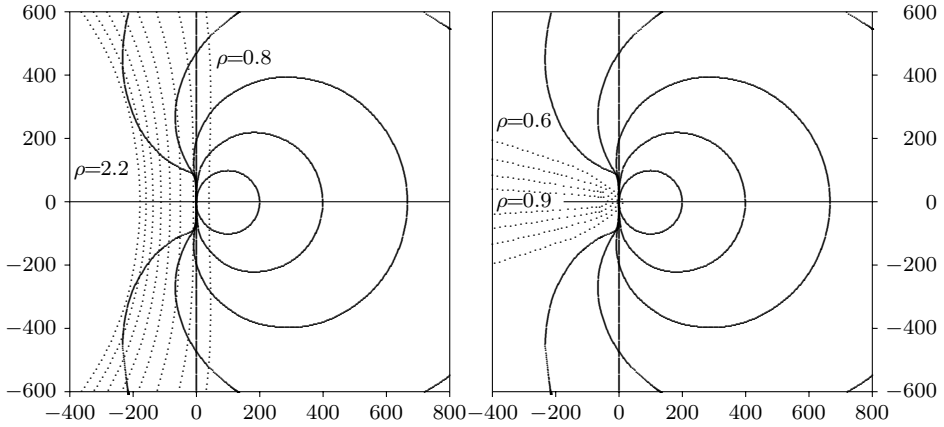

FIG. 5.3. *Spectral pictures of optimal double-splitting (left) and convolution (right) SOR waveform relaxation for model problem* (5.1) *with* $m = 1$ *and linear finite-element discretization* ($h = 1/16$, $\tau = 1/100$).

mesh with mesh-size $h = 1/16$. The results for finite differences or more-dimensional problems are qualitatively similar.

We computed $\rho(\mathcal{K}_\tau^{DSSOR,\omega^\star})$ by direct numerical evaluation of (4.5), with $\tau = 1/100$ and with $\Omega_\tau = \omega^\star \delta_\tau$, where $\omega^\star$ equals the optimal ω for the continuous-time iteration. Since $(\mu_1)_\tau(z) \in \mathbb{C} \setminus \{(-\infty, -1] \cup [1, \infty)\}$ and $(\mu_1)_\tau(z)$ is analytic for $|z| \geq 1$, we have that $(\tilde{\Omega}_{opt})_\tau(z)$, given by (4.8), is also analytic. Hence, we can also compute $\rho(\mathcal{K}_\tau^{CSOR,opt})$ by evaluation of (4.5). The results for the DSSOR and CSOR iteration are reported in Table 5.3. They can be illustrated by a so-called spectral picture, see [9, sect. 6], in which the scaled stability region boundaries of the linear multistep methods are plotted on top of the contour lines of the spectral radius of the continuous-time waveform relaxation symbol. Two such pictures are given in Figure 5.3, with contour lines drawn for the values 0.8, 1.0, 1.2, 1.4, 1.6, 1.8, 2.0, and 2.2 in the DSSOR case and 0.6, 0.7, 0.8, and 0.9 in the CSOR case. According to Theorem 4.7, the values of Table 5.3 can be verified visually by looking for the supremum of the symbol's spectral radius along the plotted scaled stability region boundaries.

5.4. Numerical results. In this section we will present the results of some numerical experiments. We will show that the observed convergence behavior agrees very well with the theory. For long enough time windows, the averaged convergence factors closely match the theoretical spectral radii on infinite time intervals. For an explanation of why they do not agree with the *finite*-interval ones, we refer to [9, sect. 7.1] and to the pseudo-spectral analysis of [7], [16]. To determine the averaged convergence factor, we first computed the νth iteration convergence factor by calculating the l_2-norm of the discrete error of the νth approximation $u_\tau^{(\nu)}$ and by dividing the result

for successive iterates. This factor takes a nearly constant value after a sufficiently large number of iterations. The averaged convergence factor is then defined as the geometric average of these iteration convergence factors in the stable regime.

For the problems already discussed in this section, the Z-transform of the optimal convolution kernel is known to be analytic for $|z| \geq 1$ and is given by (4.8). The computation of the components $\Omega_{opt}[n]$ of the optimal discrete convolution kernel, which satisfy

$$(\tilde{\Omega}_{opt})_\tau(z) = \sum_{n=0}^{\infty} \Omega_{opt}[n] z^{-n}, \tag{5.12}$$

involves the use of an inverse Z-transform technique. The method we used is based on a Fourier-transform method, and is justified by the following observation. Setting $\bar{\Omega}(t) = (\tilde{\Omega}_{opt})_\tau(e^{-it})$, (5.12) becomes

$$\bar{\Omega}(t) = \sum_{n=0}^{\infty} \Omega_{opt}[n] e^{int}.$$

Thus, $\Omega_{opt}[n]$ is the n-th Fourier coefficient of the 2π-periodic function $\bar{\Omega}(t)$. More precisely,

$$\Omega_{opt}[n] = \frac{1}{2\pi} \int_0^{2\pi} \bar{\Omega}(t) e^{-int} dt,$$

which can be approximated numerically by the finite sum

$$\Omega_{num}[n] = \frac{1}{M} \sum_{k=0}^{M-1} \bar{\Omega}\left(k \frac{2\pi}{M}\right) e^{-ink\frac{2\pi}{M}}.$$

Consequently, numerical approximations to the M values $\{\Omega_{opt}[n]\}_{n=0}^{M-1}$ can be found by computing the discrete Fourier transform of the sequence $\{(\tilde{\Omega}_{opt})_\tau(e^{-ik\frac{2\pi}{M}})\}_{k=0}^{M-1}$. This can be performed very efficiently by using the FFT-algorithm. In the numerical experiments the number of time steps N is always finite. Hence, we only use the numerical approximations of $\{\Omega_{opt}[n]\}_{n=0}^{N-1}$. To compute the discrete kernel, we took $M \geq N$ and large enough to anticipate possible aliasing effects.

The correctness of formulae (3.14) and (3.15) is illustrated in Figure 5.1 by the "+"- and the "×"-symbols. They correspond to the measured averaged convergence factors of the SSSOR and DSSOR waveform relaxation method, respectively, applied to the one-dimensional model problem (5.1). In this computation the time window equals $[0, 1]$, the time step τ is $1/1000$ and the time discretization is by the Crank–Nicolson method.

Averaged convergence factors as a function of h are given in Tables 5.4 and 5.5 for the one- and two-dimensional model problem (5.1). They agree very well with the theoretical values given in Table 5.1, and they illustrate the correctness of formulae (5.3), (5.4), and (5.5). Note that we take the overrelaxation parameters ω in the numerical experiments equal to the optimal parameters ω_{opt} of the corresponding continuous-time iterations; see also section 5.3.

In order to illustrate the dramatic improvement of convolution SOR over the other SOR waveform relaxation methods we included Figure 5.4. There, we depict the evolution of the l_2-norm of the error as a function of the iteration index. The results for

TABLE 5.4
Averaged convergence factors of optimal SSSOR, DSSOR, and CSOR waveform relaxation for model problem (5.1) *with* $m = 1$, *finite-difference discretization, and Crank–Nicolson method* ($\tau = 1/100$). *Compare with Table* 5.1.

h	1/8	1/16	1/32	1/64
SSSOR	0.713	0.919	0.979	0.995
DSSOR	0.783	0.942	0.985	0.996
CSOR	0.441	0.676	0.820	0.907

TABLE 5.5
Averaged convergence factors of optimal SSSOR, DSSOR, and CSOR waveform relaxation for model problem (5.1) *with* $m = 2$, *finite-difference discretization, and Crank–Nicolson method* ($\tau = 1/100$). *Compare with Table* 5.1.

h	1/8	1/16	1/32	1/64
SSSOR	0.718	0.921	0.980	0.995
DSSOR	0.788	0.944	0.986	0.996
CSOR	0.442	0.670	0.822	0.909

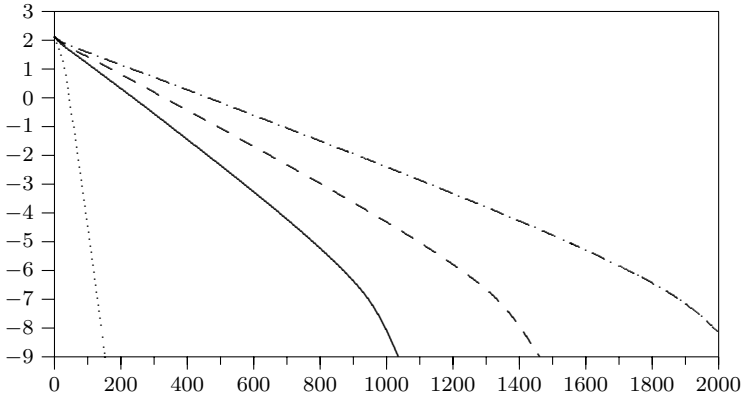

FIG. 5.4. $\log ||e_\tau^{(\nu)}||_2$ *vs. iteration index* ν *for model problem* (5.1) *with* $m = 2$, *finite-difference discretization, and Crank–Nicolson method* ($h = 1/32$, $\tau = 0.01$), *using Gauss–Seidel (dash-dotted), SSSOR (solid), DSSOR (dashed), and CSOR (dotted) waveform relaxation.*

standard Gauss–Seidel waveform relaxation are also given. Observe that qualitatively similar convergence plots are obtained for certain nonlinear semiconductor device problems in [21, sect. 7.2].

The correctness of (5.7) is illustrated in Figure 5.2 where the "+"-symbols correspond to observed averaged convergence factors for the double-splitting SOR waveform relaxation method, applied to the one-dimensional model problem (5.1) with linear finite-element discretization, time window $[0, 1]$, $\tau = 1/1000$, and Crank–Nicolson time discretization. In Table 5.6 we present numerical results as a function of h for optimal DSSOR and CSOR waveform relaxation. These values should be compared to the ones given in Table 5.2. Moreover, the CSOR results illustrate the correctness of (5.11). Finally, averaged convergence rates obtained with different time-discretization formulae are given in Table 5.7. They match the theoretical values of Table 5.3 very well.

TABLE 5.6
Averaged convergence factors of optimal DSSOR and CSOR waveform relaxation for model problem (5.1) *with* $m = 1$*, linear finite-element discretization, and Crank–Nicolson method* ($\tau = 1/100$)*. Compare with Table* 5.2.

h	1/8	1/16	1/32	1/64
DSSOR	0.817	0.952	0.988	0.997
CSOR	0.441	0.676	0.819	0.908

TABLE 5.7
Averaged convergence factors of optimal DSSOR and CSOR waveform relaxation for model problem (5.1) *with* $m = 1$*, linear finite-element discretization,* ($h = 1/16$, $\tau = 1/100$)*. Compare with Table* 5.3.

multistep method	CN	BDF(1)	BDF(2)	BDF(3)	BDF(4)	BDF(5)
DSSOR	0.953	0.953	0.953	0.965	1.221	2.142
CSOR	0.637	0.637	0.632	0.630	0.630	0.629

6. Linewise CSOR waveform relaxation. A finite-element discretization of model problem (5.1) does not in general lead to matrices $zB + A$ that are consistently ordered for pointwise relaxation. These matrices may, however, be consistently ordered for blockwise or linewise relaxation. As an illustration, we investigate the performance of linewise CSOR waveform relaxation for the finite-element discretization of the two-dimensional heat equation. The relevant stencils are given by

$$B = \frac{h^2}{12}\begin{bmatrix} & 1 & 1 \\ 1 & 6 & 1 \\ 1 & 1 & \end{bmatrix} \quad \text{and} \quad A = \begin{bmatrix} & -1 & \\ -1 & 4 & -1 \\ & -1 & \end{bmatrix}$$

in the linear finite-element case and by

$$B = \frac{h^2}{36}\begin{bmatrix} 1 & 4 & 1 \\ 4 & 16 & 4 \\ 1 & 4 & 1 \end{bmatrix} \quad \text{and} \quad A = \frac{1}{3}\begin{bmatrix} -1 & -1 & -1 \\ -1 & 8 & -1 \\ -1 & -1 & -1 \end{bmatrix}$$

in the bilinear finite-element case. We also study the linewise CSOR method for the finite-difference discretization of the two-dimensional model problem (5.1).

The resulting matrices $zB + A$ are block-consistently ordered and, therefore, the Young relation (3.10) holds. Unfortunately, however, the eigenvalues of the Jacobi symbols $\mathbf{K}^{\mathbf{JAC}}(z)$ are in general not collinear (except for $z = 0$ and $z = \infty$). Consequently, formula (3.12) is not guaranteed to give the optimal convolution kernel. Moreover, we cannot use Theorem 3.4 to estimate the spectral radii of the linewise CSOR waveform relaxation methods since the largest-magnitude eigenvalue $\mu_1(z)$ and, hence, $\tilde{\Omega}(z)$ are not known to be analytic for $\mathrm{Re}(z) \geq 0$.

Despite similar violations of the assumptions of Theorem 4.4 and Lemma 4.5, we used formula (4.8) to compute the convolution sequence $(\Omega_{num})_\tau = \{\Omega_{num}[n]\}_{n=0}^{N-1}$, following the procedure explained in section 5.4. That is, we compute $(\mu_1)_\tau(z)$ for M values of z located equidistantly along the unit circle. We apply (4.8) to compute the corresponding values of $\tilde{\Omega}_\tau(z)$, or, $\bar{\Omega}(t)$, and we compute the Fourier transform of this sequence to arrive at M values $\Omega_{num}[n]$, $n = 0, \ldots, M-1$. As we take M such that $M \geq N$, we truncate the sequence after the first N components. This corresponds to

TABLE 6.1

Averaged convergence factors of linewise CSOR waveform relaxation for model problem (5.1) *with* $m = 2$ *and Crank–Nicolson time discretization* ($\tau = 1/100$). *The theoretical spectral radii of the corresponding standard linewise SOR method are given in parenthesis.*

h	1/8	1/16	1/32	1/64
finite differences	0.318 (0.322)	0.568 (0.572)	0.756 (0.757)	0.871 (0.870)
linear finite elements	0.320 (0.322)	0.569 (0.572)	0.757 (0.757)	0.870 (0.870)
bilinear finite elements	0.312 (0.317)	0.567 (0.571)	0.760 (0.757)	0.870 (0.870)

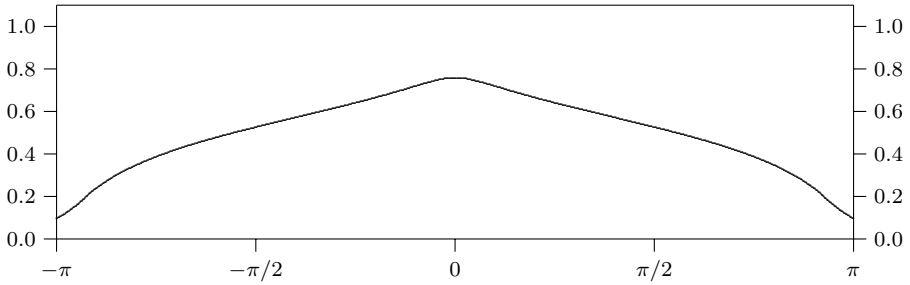

FIG. 6.1. $\rho(\mathbf{K}_\tau^{\mathbf{CSOR}}(e^{i\theta}))$ *for linewise relaxation vs.* θ *for model problem* (5.1) *with* $m = 2$ *and linear finite-element discretization* ($h = 1/32$).

TABLE 6.2

$\rho(\mathbf{K}_\tau^{\mathbf{CSOR}}(e^{i\theta}))$ *for linewise relaxation as a function of* θ *for model problem* (5.1) *with* $m = 2$ *and linear finite-element discretization* ($h = 1/32$).

θ	0	0.01	0.02	0.03	0.04	0.05	0.06
$\rho(\mathbf{K}_\tau^{\mathbf{CSOR}}(e^{i\theta}))$	0.757	0.759	0.761	0.761	0.760	0.759	0.756

using an $l_1(\infty)$-kernel of the form

$$(\Omega_{num})_\tau = \{\Omega_{num}[0], \Omega_{num}[1], \ldots, \Omega_{num}[N-1], 0, 0, \ldots, 0, \ldots\}. \tag{6.1}$$

Numerical results, based on Crank–Nicolson time discretization with time step $\tau = 1/100$, are reported in Table 6.1. We also included the theoretical spectral radii of the optimal linewise SOR method for the corresponding linear systems $Au = f$. Observe that the latter, which can be approximated by $1 - 2\sqrt{2}\pi h$ for small mesh-size h, [3, p. 152], agree very well with the averaged convergence factors of the linewise CSOR waveform relaxation methods.

To illustrate and explain this behavior we provide Figure 6.1, where we depict $\rho(\mathbf{K}_\tau^{\mathbf{CSOR}}(e^{i\theta}))$, $\theta \in [-\pi, \pi]$, for the two-dimensional heat equation, discretized using linear finite elements on a mesh with mesh-size $h = 1/32$. From this picture it is clear that the maximum in (4.5) is found very close to $\theta = 0$ (or $z = 1$). The maximum is not exactly at the origin though, as we see from Table 6.2 where values of $\rho(\mathbf{K}_\tau^{\mathbf{CSOR}}(e^{i\theta}))$ are presented for θ close to 0.

By construction, $\bar{\Omega}(0)$ equals the optimal overrelaxation parameter for the linewise SOR method applied to the problem $Au = f$. By definition of the inverse Fourier

transform, we have that

$$\bar{\Omega}(0) = \sum_{n=0}^{M-1} \Omega_{num}[n]. \tag{6.2}$$

Because of the rapid decay of the Fourier coefficients, the latter is a very good approximation of the Z-transform of (6.1) at $z = 1$, $(\tilde{\Omega}_{num})_\tau(1)$, if $M > N$. In particular, (6.2) equals $(\tilde{\Omega}_{num})_\tau(1)$ if $M = N$. Hence, in Figure 6.1, the value of the spectral radius of the optimal linewise SOR method for the stationary problem (or a very good approximation to it) is found at the origin. Since the curve peaks close to the origin, we may expect a similar convergence rate for the linewise CSOR waveform relaxation method as for the optimal linewise SOR method for the system $Au = f$.

7. Conclusions. In this paper, we gave an overview of the different SOR waveform relaxation methods for general ODE systems of the form $B\dot{u} + Au = f$. The methods using a single scalar parameter were shown to lead to some acceleration. This acceleration is, however, only a marginal one. The method based on convolution, using a frequency-dependent overrelaxation parameter, proved to be vastly superior, leading to a convergence acceleration similar to the convergence acceleration of the optimal SOR method for solving stationary problems.

It was our aim in this paper to provide the theoretical framework in which to study the different SOR waveform methods, and to illustrate the potential convergence acceleration of the convolution method. We realize that in order to cast the latter into a practical procedure more research is required, in particular on how to derive the optimal overrelaxation kernel. For stationary problems, the determination of a good overrelaxation parameter ω is already nontrivial. Finding a good convolution kernel for time-dependent problems is expected to be even far more difficult. Yet, the problem does not seem to be insurmountable. Some promising results have already been reported in [21], where an automatic procedure is developed for determining a good $\Omega(t)$. In addition, our results in section 6 show that the lemmas concerning the optimal convolution kernel, i.e., Lemmas 3.6 and 4.5 appear to be "robust." That is to say, even though some assumptions are violated, the use of a convolution kernel based on the former lemmas leads to an excellent convergence acceleration.

Acknowledgments. The authors would like to thank Min Hu, Ken Jackson, Andrew Lumsdaine, Ulla Miekkala, and Mark W. Reichelt for many helpful discussions and an anonymous referee for several suggestions which substantially improved the quality and structure of the paper.

REFERENCES

[1] A. Bellen, Z. Jackiewicz, and M. Zennaro, *Contractivity of waveform relaxation Runge–Kutta iterations and related limit methods for dissipative systems in the maximum norm*, SIAM J. Numer. Anal., 31 (1994), pp. 499–523.

[2] A. Bellen and M. Zennaro, *The use of Runge-Kutta formulae in waveform relaxation methods*, Appl. Numer. Math., 11 (1993), pp. 95–114.

[3] G. Birkhoff and R. E. Lynch, *Numerical Solution of Elliptic Systems*, Vol. 6, SIAM Stud. Appl. Math., SIAM, Philadelphia, 1984.

[4] R. Curtain and A. Pritchard, *Functional Analysis in Modern Applied Mathematics*, Academic Press, London, 1977.

[5] K. Hoffman, *Banach Spaces of Analytic Functions*, Prentice–Hall, Englewood Cliffs, NJ, 1962.

[6] M. Hu, K. Jackson, and B. Zhu, *Complex Optimal SOR Parameters and Convergence Regions*, Working Notes, Department of Computer Science, University of Toronto, Ontario, Canada, 1995.

[7] Z. Jackiewicz and B. Owren, *Convergence analysis of waveform relaxation methods using pseudospectra*, Tech. Report Numerics 2, Department of Mathematics, University of Trondheim, Norway, 1995.
[8] J. Janssen and S. Vandewalle, *Multigrid waveform relaxation on spatial finite-element meshes: The continuous-time case*, SIAM J. Numer. Anal., 33 (1996), pp. 456–474.
[9] J. Janssen and S. Vandewalle, *Multigrid waveform relaxation on spatial finite-element meshes: The discrete-time case*, SIAM J. Sci. Comput., 17 (1996), pp. 133–155.
[10] G. S. Jordan, O. J. Staffans, and R. L. Wheeler, *Local analyticity in weighted L^1-spaces and applications to stability problems for Volterra equations*, Trans. Am. Math. Soc., 274 (1982), pp. 749–782.
[11] B. Kredell, *On complex successive overrelaxation*, BIT, 2 (1962), pp. 143–152.
[12] J. D. Lambert, *Computational Methods in Ordinary Differential Equations*, John Wiley and Sons, Chichester, 1973.
[13] C. Lubich, *Chebyshev acceleration of Picard-Lindelöf iteration*, BIT, 32 (1992), pp. 535–538.
[14] C. Lubich and A. Ostermann, *Multi-grid dynamic iteration for parabolic equations*, BIT, 27 (1987), pp. 216–234.
[15] A. Lumsdaine, *Theoretical and Practical Aspects of Parallel Numerical Algorithms for Initial Values Problems, with Applications*, Ph.D. thesis, Department of Electrical Engineering and Computer Science, Massachusetts Institute of Technology, Cambridge, MA, 1992.
[16] A. Lumsdaine and D. Wu, *Spectra and pseudospectra of waveform relaxation operators*, SIAM J. Sci. Comput., 18 (1997), pp. 286–304.
[17] U. Miekkala and O. Nevanlinna, *Convergence of dynamic iteration methods for initial value problems*, SIAM J. Sci. Statist. Comput., 8 (1987), pp. 459–482.
[18] U. Miekkala and O. Nevanlinna, *Sets of convergence and stability regions*, BIT, 27 (1987), pp. 554–584.
[19] W. Niethammer and R. Varga, *The analysis of k-step iterative methods for linear systems from summability theory*, Numer. Math., 41 (1983), pp. 177–206.
[20] A. D. Poularakis and S. Seely, *Elements of Signals and Systems*, PWS-Kent Series in Electrical Engineering, PWS-Kent Publishing Company, Boston, 1988.
[21] M. W. Reichelt, J. K. White, and J. Allen, *Optimal convolution SOR acceleration of waveform relaxation with application to parallel simulation of semiconductor devices*, SIAM J. Sci. Comput., 16 (1995), pp. 1137–1158.
[22] R. Skeel, *Waveform iteration and the shifted Picard splitting*, SIAM J. Sci. Stat. Comput., 10 (1989), pp. 756–776.
[23] V. Thomée, *Galerkin Finite Element Methods for Parabolic Problems*, Lecture Notes in Math., 1054, Springer-Verlag, Berlin, 1984.
[24] S. Vandewalle, *Parallel Multigrid Waveform Relaxation for Parabolic Problems*, B.G. Teubner, Stuttgart, 1993.
[25] R. S. Varga, *Matrix Iterative Analysis*, Prentice-Hall, Englewood Cliffs, NJ, 1965.
[26] S. Wolfram, *Mathematica, a System for Doing Mathematics by Computer*, Addison–Wesley, New York, 1988.
[27] D. M. Young, *Iterative Solution of Large Linear Systems*, Academic Press, New York, 1971.